JOURNAL OF MATERIALS SCIENCE **36** (2001) 3891 – 3896

Porosity determinations in thermally sprayed hydroxyapatite coatings

C. E. MANCINI, C. C. BERNDT*, L. SUN, A. KUCUK
Department of Materials Science and Engineering, The State University of New York at Stony Brook, Stony Brook, NY 11794, USA
E-mail: cberndt@notes.cc.sunysb.edu

The porosity of various thermally sprayed coatings was determined using an Archimedian Method. The method relies on density determinations and buoyancy effects. First, measurements were carried out on standard samples in order to verify the accuracy and reliability of the Archimedian method. Then, porosity measurements were taken for hydroxyapatite samples and correlated to its physical properties. The results from the experiments show that as the crystallinity of the HAp increases, the porosity increases. Also, as the amorphous content increases, porosity decreases. Other relationships indicated that the porosity decreased as the stand off distance increased and it decreased with a power increase.

1. Introduction

Hydroxyapatite (HAp) is an example of a bioactive material, which can be thermally sprayed. Such coatings have been used as a surface coating on metallic implants in dentistry and orthopedics since the mid 1980's [1, 2]. The attributes of HAp include (i) more rapid fixation and stronger bonding between the host bone and the implant and (ii) increased uniform bone ingrowth and/or ongrowth at the bone implant interface [3–5]. Not all clinical trials have demonstrated significant benefit of HA-coated implants [6–8]. However, many trials with either weight-bearing or non-weight-bearing models have shown promising results shortly after the implantation and continued fixation for up to 10 years [9–13].

The importance of HAp has increased due to the need to improve the quality and reliability of patient care. The HAp composition is very similar to the composition of bone; therefore, hydroxyapatite coatings can be used in many applications for the expeditious healing and fixation of orthopedic implants. The properties and reaction of HAp have become increasingly more important as the possibilities for its use and benefits increase. In addition, any aspects of the material that may contribute to its performance within the human body, such as porosity, are considerably meaningful [14].

Porosity influences the physical and mechanical characteristics of hydroxyapatite. Porosity also affects the body's reaction to this mineral component of bone. The rate of bone ingrowth and the rate of dissolution will be increased by the porosity of the hydroxyapatite [15]. This allows the establishment of a stronger interface between the bone and prosthesis. The porous structure permits fibrovascular ingrowth, helping the implant resist migration [16]. On the other hand, high porosity will affect the mechanical strength of the hydroxyapatite. If the hydroxyapatite contains a high volume of larger, interconnected pores, then the mechanical strength of the hydroxyapatite will be greatly diminished [17]. A balance in the porosity should be established where the strength of the material will be compromised just enough to ensure the best reaction with the body; thereby creating a secure interface between the bone and the prosthesis.

All thermally sprayed coatings have some degree of porosity. The process involves melting the particles to sufficiently high temperatures to create a coating that will adhere to the substrate. Melted splats of particles will compact into a coating, which will have different densities and porosities depending upon the spray parameters [18]. The porosity of the coating is a defining physical characteristic. It is important to establish spray parameters that will provide an optimal coating which is both mechanically strong and biologically compatible. Thus, the comfort of the patient will be improved and the recovery time of the patient will be expedited.

Porosity levels are established by using various methods, which can be tedious or unreliable, such as mercury intrusion porosimetry (MIP) or image analysis (IA) techniques. The Archimedian method for measuring porosity is reliable and time efficient [19, 20]. The basis for the Archimedian method is simple. The samples are submersed in water. The samples act like a sponge, in that as air diffuses out of the sample, water will diffuse into the sample, causing the weight of the sample to increase. The pores in the sample allow for the diffusion of water. The more pores, or the larger the pores, the more weight the sample will gain. The

*Author to whom all correspondence should be addressed.

weight gain of the sample can be directly related to the volume of the pores and, therefore, the apparent porosity of the sample [21]. It is called apparent porosity because the volume is calculated by using weights of the sample, not by direct measurement. Closed or sealed pores are not included in the apparent porosity value. The apparent porosity values are usually close to the total porosity as long as the closed porosity in the sample is low.

In this study, the objective was to develop an accurate technique to measure porosity. Then, use this technique to measure the porosity of HAp coatings and finally, to correlate the phase of hydroxyapatite and mechanical properties to its porosity. The ultimate goal is to engineer a coating which is designed to maximize the bioactivity and resorption of the hydroxyapatite, in order to optimize the clinical application.

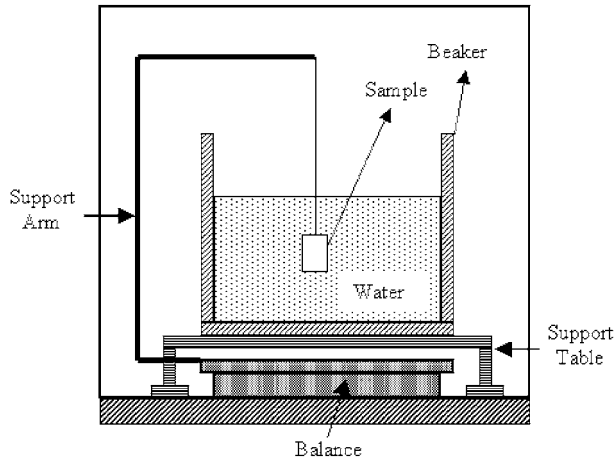

Figure 1 Experimental apparatus used to measure the weight of the sample in water.

2. Experimental procedure

2.1. Sample preparation

HAp coatings were air plasma sprayed using a Metco 3MB plasma torch with a Metco GH nozzle (Sulzer-Metco, Westbury, NY-USA) mounted on a six-axis articulated robot (Model S400, GMF Fanuc, Chartlotteville, VA-USA). The details of HAp coating preparation were given elsewhere [22, 23]. A PAL-160 Water Stabilized Plasma system (The Institute of Plasma Physics, Prague, The Czech Republic) [24, 25] was used to produce 5 weight percent CaO-ZrO_2 and spinel ($MgAl_2O_4$) free standing coatings.

Four samples of hydroxyapatite prepared under different spray parameters (Table I) were tested. The powder was spherical ranging from 10–120 um with a normalized size distribution averaging 45 um [22]. Samples B and D were sprayed at a lower power level than the plasma level employed with samples F and H. Also, samples B and F were sprayed at a shorter stand off distance than samples D and H.

2.2. Porosity measurements

The porosity was measured using the Archimedian method and ASTM C 373 − 88 was used as a guide for the experimental method [21]. The freestanding samples range in volume between 1 mm^3 to 100 mm^3. The first step in the procedure was to dry the samples in an oven at 150°C. A dry weight was established by weighing the samples until a stable weight was reached. A Mettler Toledo balance with ±0.01 mg accuracy was used in this experiment. The samples were generally dried in the oven for 12–24 hours. Then the samples were soaked in water at ambient temperature and weighed in air and in water. The soaking time of samples was a variable such that the measurements were determined when the value of the weight stabilized. Therefore, at this point in time the soaking samples could be measured in the water. The weight in water was measured by harnessing the sample in a device, shown in Fig. 1, which suspended the sample in water. The balance would measure the weight of the support arm and sample, not the weight of the water. Therefore, if the support arm has a known weight, then the weight of the wet sample alone can be obtained. The water was supported on a bench, which sat on the outside of the balance pan to ensure the independence of the water from the balance thereby allowing the most precise measurement.

TABLE I Spray parameters of the four different HAp samples

Parameters	HA-B	HA-D	HA-F	HA-H
Current (A)	500	500	600	600
Voltage (V)	55	55	70	70
Primary Gas, Ar (slpm)	50	50	50	50
Secondary Gas, H2 (slpm)	6	6	13	13
Carrier Gas, Ar (slpm)	3.65	3.65	3.65	3.65
Power (kW)	27.5	27.5	42	42
Stand off Distance (mm)	80	160	80	160
Powder Feeding rate (g/min)	14	14	14	14

The samples were suspended in water until a constant weight was established. For the hydroxyapatite samples it was found that the samples should be suspended for approximately 24–52 hours in order for the porosity to stabilize. The porosity can be measured from the sample weights. If the samples dissolve or exhibit areas where there has been some chipping of the sample, another dry weight can be established after the conclusion of the experiment. Therefore, after the wet weights were found, then the samples can be returned to the oven. The samples were dried until a constant weight was achieved and then reweighed. This weight can be used as the new dry weight.

The weights of the samples are used to obtain densities as well as apparent porosity. A volume of the sample is obtained in various ways to measure differing aspects of the coating. For example, the exterior volume is obtained by taking the wet mass in air and subtracting the wet mass in water. The porosity is calculated by taking the wet mass in air and subtracting the dry mass. This number is then divided by the exterior volume and converted to the percent apparent porosity by using Equation 1; where P is the apparent percent porosity, M is the saturated mass or wet mass in air, D is the dry mass and V is the exterior volume, calculated as $V = M - S$, where S is the mass while suspended in

water or the wet mass in water.

$$P = \left(\frac{M - D}{V}\right) \times 100 \quad (1)$$

2.3. Physical properties

The samples were also tested for their mechanical properties and chemistry so that the porosity results could be correlated to the sample properties. The average roughness, R_a of the samples was measured using a Hommel T1000 mechanical profilometer (Hommel America, New Britain, CT-USA). The measurements were carried out along two orthogonal directions with a 0.5 mm/s traverse according to ISO 4287 standard procedure [26]. The Vickers hardness was determined with a Tukon Microhardness tester (Instron, Canton, MA-USA). The measurements were performed on the polished cross section of the samples at a 50 g load for 15 seconds.

2.4. Phase analysis

The hydroxyapatite coatings underwent phase analysis. The x-ray diffraction of the HAp coatings was the primary technique used to determine the structure and phase. X-ray diffraction measurements were carried out using a computerized Philips PW 1729 X-ray diffractometer with CuK_α radiation, 40 kV voltage and 30 mA current. The samples were scanned at a rate of 0.005 °/sec over a 2θ range of 20° to 60°. Further details of measurements have been presented previously [22, 23].

3. Results and discussion

3.1. Reference porosity measurements

The porosity was first measured on samples of 5 wt% calcia partially stabilized zirconia (PSZ) and spinel ($MgAl_2O_4$). These samples had known porosity and, therefore, were used as standards to validate the technique. The samples were first measured by MIP (Mercury Intrusion Porosimetry). The Archimedian method measured apparent porosities of 5.8%, 7.1%, and 6.7% with an average of $6.5 \pm 0.67\%$. The results obtained were consistent with each other. For the MIP results 3 to 5 samples were tested and an average of $5.9 \pm 0.5\%$ was obtained. This result correlates well with prior studies [27] and indicates that the Archimedian method is suitable.

The porosity of the partially stabilized zirconia samples was also found using the Archimedian technique. The results for two samples, Fig. 2, indicate that the values derived via the Archimedian method initially increased to the MIP value as more water intruded into the samples. The porosity of the zirconia samples from MIP was calculated to be $11.8 \pm 0.5\%$ [19]. The measured porosity for the samples rose to $11.6 \pm 0.2\%$ and $12.3 \pm 0.2\%$, respectively. Again these results were consistent with each other and with the MIP results.

Since the results from the spinel and stabilized zirconia samples were consistent with previously found reliable results, the Archimedian technique for measuring porosity proved to be accurate and reliable. The Archimedian method for measuring porosity is reliable, convenient, inexpensive, uncomplicated, and safe.

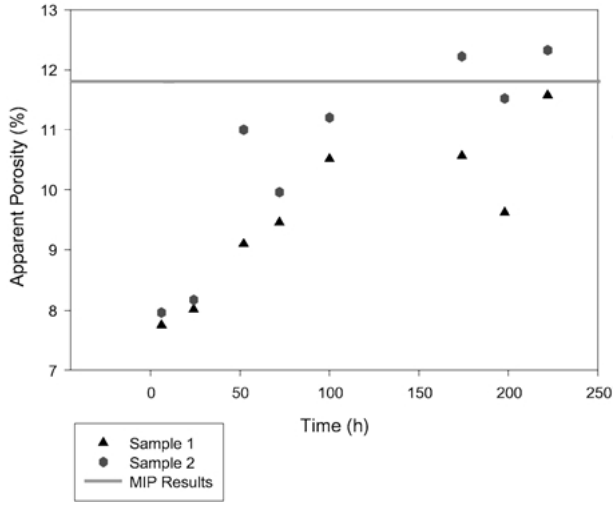

Figure 2 Porosity measurements of partially stabilized zirconia samples.

3.2. Phase analysis of HAp coatings

The X-ray diffraction patterns taken from the surfaces of HAp coatings can be seen in Fig. 3a–d. In general, coatings B and F are more crystalline, while coatings H and D are more amorphous. The XRD with more defined distinct peaks are the more crystalline. The diffraction patternss for the more amorphous coatings have a hump resulting from the presence of an amorphous phase. The peaks are less distinctive due to the presence of the amorphous phase.

The detailed analysis of XRD patterns revealed that sprayed coatings were a mixture of amorphous calcium phosphate (ACP), tricalcium phosphate, tetracalcium phosphate, calcium oxide, and hydroxyapatite phases [22, 23]. This is very different from the original feedstock, which was 100% crystalline hydroxyapatite. It was suggested that HAp decomposes into other phases under the harsh plasma environment [22, 23]. The phase distribution for each sample was examined in detail elsewhere, but it is summarized in Table II. The relative error in the calculations is within five percent of the average value shown on Table II [22]. The phase distribution on the surface of the coatings and coating substrate interface are represented as "S" and "I", respectively.

As shown in Table II, the percentage of crystalline HAp decreased with increasing torch power and stand off distance. When a HAp particle was introduced into the plasma flame, the particle was either melted or partially melted; the higher the torch power the higher the amount of melting. A torch operated with a high power generates a plasma flame with a higher temperature. The molten HAp particle can stay as pure HAp or decompose to form phases such as tricalcium phosphate (TCP), tetracalcium phosphate (TTCP), and calcium oxide (CaO) depending on the flame conditions.

TABLE II Summary of the phase distribution identified for each hydroxyapatite sample. The phase distribution on the surface of the coatings and coating substrate interface are represented as "S" and "I", respectively

	HA-B (%)		HA-D (%)		HA-F (%)		HA-H (%)	
Phases	S	I	S	I	S	I	S	I
Amorphous Calcium Phosphate	10	27	46	66	15	48	52	69
Tricalcium Phosphate	10	7	10	6	15	2	11	4
Tetracalcium Phosphate	4	3	3	3	9	4	5	2
Calcium Oxide	5	12	3	3	15	32	19	22
Hydroxyapatite	71	49	38	22	46	14	13	3

For example, the depletion of hydrogen results in either TCP or TTCP formation, while volatilization of P_2O_5 and depletion of hydrogen leads to formation of CaO. Therefore, a high torch power, which allows higher in-flight particle temperatures, would create a coating which contains less crystalline HAp as seen in Table II. A molten particle solidifies as either crystalline or amorphous phase depending on the cooling rate. A higher cooling rate promotes formation of an amorphous phase. As seen in Table II, the percentage of amorphous phase is higher near the substrate-coating interface. The rate of cooling is higher near the interface because the metal substrate has a high thermal conductivity and, therefore, behaves as a heat sink. However, as the splats build-up on each other, the heat dissipation rate decreases resulting in a lower cooling rate and a crystalline phase.

When a particle is injected into a plasma flame, the particle heats up as a result of heat exchange between the flame and particle to a certain temperature. As the particle moves further away from the flame, the temperature starts decreasing. Therefore, the particle temperature may be lower for a greater stand off distance. In addition, a larger stand off distance provides a longer residence time in the flame resulting in a longer time for the melting of the HAp particles. Therefore, the crystalline HAp is lower for the coatings sprayed at a larger stand off distance. As seen in Table II, the amorphous phase content is higher for the coatings sprayed at longer stand off distance because the particle temperature is lower at a stand off distance of 160 mm than at 80 mm. This lower temperature provides a greater cooling rate and results in an amorphous phase. The larger cooling rate is an effect of the low temperature gradient between the particle in flight and the substrate or room temperature. Therefore, as the stand off distance increases, the amorphous content increases.

3.3. Properties of HAp coatings

3.3.1. Porosity

The apparent porosity was measured for each of these samples and the results can be seen in Fig. 4. The porosity of sample B is 12.0%, while sample F, whose spray parameters are the same as sample B except for the power, is 7.1%. Similarly, the porosity of sample D is 5.1% and sample H has a porosity of 3.0%. It was found that there is a direct relationship between the porosity and the phase of the HAp coatings. Samples B and F are the more crystalline samples; and they also exhibit a higher porosity than samples D and H. These samples with a higher porosity were sprayed at the lower stand off distance of 80 mm. Also, the samples with a lower power of 27.5 kW have a higher porosity than the samples with a power of 42 kW. Samples B and D were prepared at a lower power than samples F and H. As the crystallinity increases, porosity increases. In contrast, as the amorphous content increases, porosity decreases. The amorphous phase does not have a distinct melting temperature like its crystalline counterpart, but rather exhibits a glass transition range. This amorphous phase can exhibit a viscous flow at temperatures much lower than the melting temperature of the crystalline counterpart, which helps to fill the pores and voids between neighbouring splats. Therefore, porosity will be lower for coatings with amorphous phases.

TABLE III The Vickers microhardness, apparent porosity, and roughness results for each of the HAp samples

Sample	Vickers Microhardness (Hv)	Porosity (%)	Roughness (R_a)
B	253 ± 60.4 (10)	12.04 ± 0.36 (3)	4.43 ± 0.92 (10)
D	277 ± 59.35 (15)	5.07 ± 1.52 (3)	6.75 ± 0.73 (10)
F	437 ± 59.8 (15)	7.07 (1)	7.59 ± 0.55 (10)
H	388 ± 47.25 (15)	3.03 (1)	5.51 ± 0.54 (10)

Note: The number in the parenthesis represents the sample size.

3.3.2. Hardness

The Vickers hardness of coatings sprayed with varying spray conditions is presented in Table III. Porosity was compared to the Vickers hardness and coating roughness. It was hypothesized that the coatings with the higher porosity would exhibit a lower hardness. However, no direct simple relationship exists between hardness and porosity values for the coatings studied. The reason is that one should also consider the phase distribution throughout the coatings since different phases have different hardness values. As seen in Tables II and III, the presence of CaO in large quantities increases hardness significantly.

On the other hand, the presence of the amorphous phase lowers the hardness as seen in sample F *versus* H. Samples F and H have approximately the same amount of CaO, but sample F has a much lower amount of the amorphous phase than sample H. Sample F has a higher microhardness than sample H. Therefore, the hardness decreases with increasing amorphous phase. Samples F and H have a high hardness because the quantity of CaO is high. Sample B has the lowest hardness because it has the highest porosity and a lower percentage of CaO

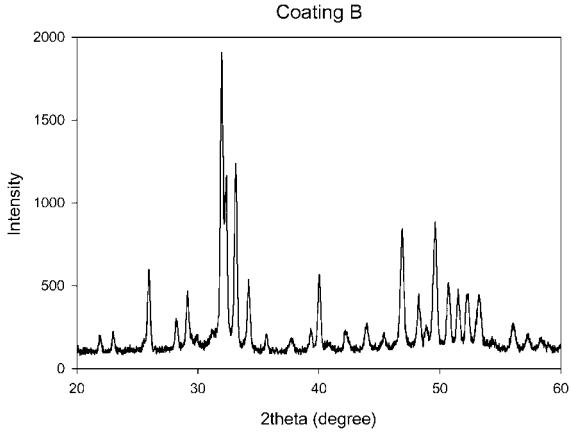

(a)

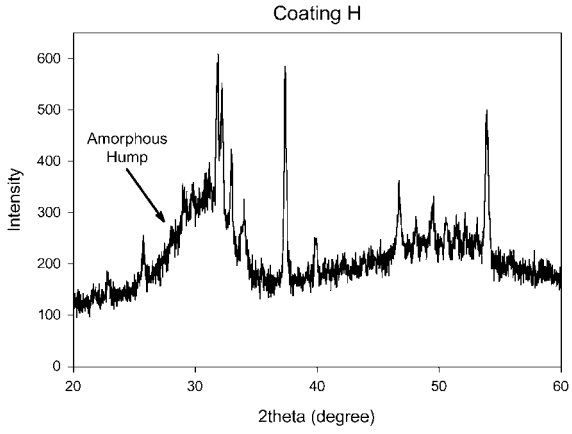

(b)

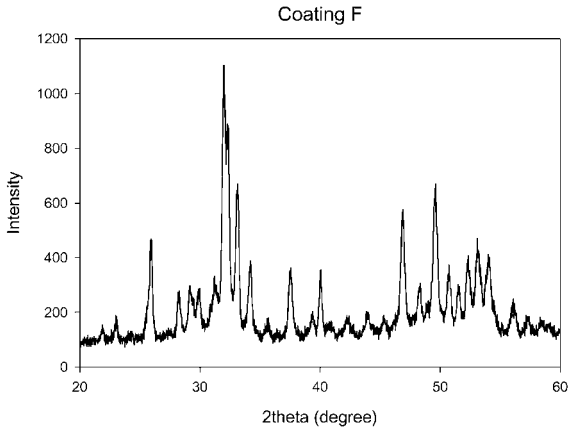

(c)

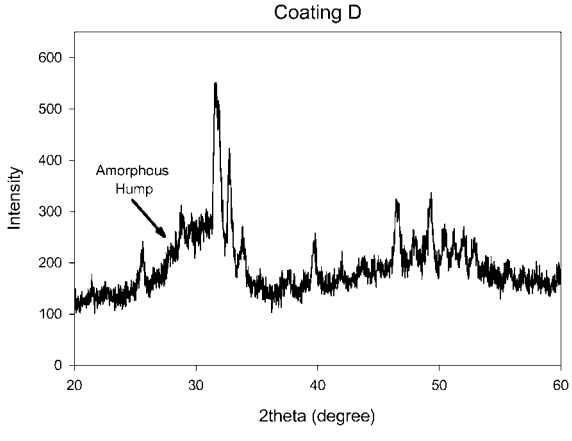

(d)

Figure 3 (a) X-ray diffraction patterns of hydroxyapatite coating B; (b) X-ray diffraction patterns of hydroxyapatite coating H; (c) X-ray diffraction patterns of hydroxyapatite coating F; (d) X-ray diffraction patterns of hydroxyapatite coating D.

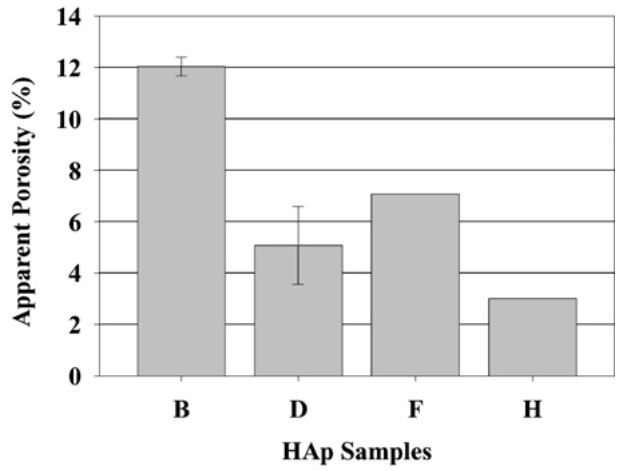

Figure 4 The bar graph representing the apparent porosity of the hydroxyapatite samples (B, D, F, and H) calculated by using the Archimedian technique.

even though it exhibits the highest amount of HAp content and lowest amount of amorphous phase(s). Sample D has a high quantity of amorphous phase and low percentage of CaO; therefore, it is consistent that sample D has a low hardness.

3.3.3. Roughness

The roughness, porosity, and hardness values are listed in Table III. The roughness of the samples appeared to decrease as the amorphous content increases. It follows that the more amorphous samples would have a smoother, less rough surface. The more amorphous samples are also the less porous samples. Coating H shows the lowest roughness; it also has the highest amorphous content and the lowest porosity. Therefore, there is a direct relationship between the porosity and roughness. There is also an inverse relationship between the porosity and amorphous content.

4. Concluding remarks

The Archimedian method for measuring porosity is a reliable, inexpensive, uncomplicated, and safe technique. Results obtained from porosity measurements of reference samples of spinel and stabilized zirconia show measurements that are accurate and reliable.

Porosity can be directly correlated to properties of hydroxyapatite that help to define its characteristics. Porosity measurements of HAp coatings indicate a substantial correlation between the phase constituents and porosity. As the crystallinity of the hydroxyapatite increases, the porosity also increases. Another important relationship is that the porosity decreases as the stand off distance increases. Also, as the power increases, the porosity decreases. The relationship between the hardness and porosity is more complex because of the presence of different phases of HAp. The hardness decreases with increasing amorphous phase, yet it increases with increasing calcium oxide. The lowest hardness correlates to the highest porosity and lowest percentage of calcium oxide. Finally, it was shown that there is a direct relationship between roughness and porosity.

The porosity measurements can be used to help define the most appropriate coating for *in vivo* or *in vitro* studies. The study of porosity as well as *in vitro* and *in vivo* experiments will provide knowledge involving how these materials interact with the human body. These experiments can potentially help to define the thermal spray parameters needed to manufacture an optimized HAp coating. Thus, ultimately the HAp coating can be designed so that the characteristics of the implant surface enable the most secure bond and fixation between the implant material and bone. These engineered properties would contribute to the patient's recovery as well as his comfort.

Acknowledgements

The authors (AK and CCB) acknowledge financial support from the National Science Foundation under NSF-MRSEC DMR, grant number 9632570. CM acknowledges the International Thermal Spray Association for an undergraduate scholarship and support from the WISE program at SUNY-Stony Brook. Special thanks to Matthew Gold, Anand Kulkarni, and Rogerio Lima, of SUNY-Stony Brook for their help with sample preparation. Also, a very special thanks to Anand Kulkarni for his help with the MIP results.

References

1. R. J. FURLONG and J. F. OSBORN, *J. Bone Joint Surg.* **73-B**(3) (1991) 741.
2. R. G. T. GEESINK, *Orthopedics*. **12** (1989) 1239.
3. R. G. T. GEESINK, K. DE GROOT and C. P. KLEIN, *J. Bone Joint Surg*. **70-B** (1988) 17.
4. S. D. COOK, K. A. THOMAS, J. F. DALTON, T. K. VOLKMAN, T. S. WHITECLOUD III and J. F. KAY, *J. Biomed. Mater. Res*. **26** (1992) 989.
5. P. K. STEPHENSON, M. A. FREEMAN, P. A. REVELL, J. GERMAIN, M. TUKE and C. J. PIRIE, *J. Arthroplasty*. **6** (1991) 51.
6. R. H. ROTHMAN, W. J. HOZACK, A. RANAWAT and L. R. N. MORIARTY, *J. Bone Joint Surg*. **78-A** (1996) 319.
7. E. J. MCPHERSON, L. D. DORR, T. A. GRUEN and M. T. SABERI, *Clinical Orthop*. **315** (1995) 223.
8. K. G. NILSSON, S. CAJANDER and J. KARRHOLM, *Acta Orthop Scan* **65** (1994) 212.
9. A. K. ROYNESDAL, E. AMBJORNSEN, S. STOVNE and H. R. HAANAS, *Int. J. Oral Maxillofac Implants*. **13**(4) (1998) 500.
10. W. J. DONNELLY, A. KOBAYASHI, T. W. CHIN, M. A. R. FREEMAN, H. YEO, M. WEST and G. SCOTT, *J. Bone Joint Surg*. **79-B**(3) (1997) 351.
11. W. D. CAPELLO, J. A. D'ANTONIO, J. R. FEINBERG and M. T. MANLEY, *ibid*. **79-A**(7) (1997) 1023.
12. R. G. H. H. NELISSEN, E. R. VALSTAR and P. M. ROZING, *ibid*. **80-A**(11) (1998) 1665.
13. G. MAGYAR, S. TOKSVIG-LARSEN and A. MORONI, *ibid*. **79-B**(3) (1997) 487.
14. K. A. GROSS, Ph.D. Dissertation, Materials Sci. Eng., State University of New York at Stony Brook, Stony Brook, NY, 1995. Accession Number: AAI9616759. Available from "OCLC FirstSearch," <http://www.oclc.org/firstsearch/> [December 29, 2000].
15. O. GAUTHIER, J.-M. BOULER, E. AGUADO, P. PILET and G. DACULSI, *Biomaterials* **19** (1998) 133.
16. H. C. GLEDHILL, I. G. TURNER and C. DOYLE, *ibid*. **20** (1999) 315.
17. K. D. GROOT, *Bioceramics: Material Characteristics Versus in Vivo Behavior* **523** (1988) 227.
18. L. PAWLOWSKI, "The Science and Engineering of Thermal Spray Coatings" (John Wiley and Sons, Chichester, 1995) p. 414.
19. J. ILAVSKY, Ph.D. Dissertation, Materials Sci. Eng., State University of New York at Stony Brook, Stony Brook, NY, 1994. Accession Number: AAG9500218. Available from "OCLC FirstSearch," <http://www.oclc.org/firstsearch/> [December 29, 2000].
20. K. MURAKAMI, C.-K. LIN, S.-H. LEIGH, C. C. BERNDT, S. SAMPATH, H. HERMAN, S. SODEOKA and H. NAKAJIMA, *Surface Modifications Technologies XI* (1998) 203.
21. ASTM C373-88, in 1992 Annual Book of ASTM Standards, edited by R. A. Storer (American Society for Testing Materials, Philadelphia, 1992) p. 115.
22. L. SUN, C. C. BERNDT, A. KUCUK, R. S. LIMA and K. A. KHOR, in "Thermal Spray: Surface Engineering Via Applied Research, edited by C. C. Berndt (ASM Inter. Materials Park, OH. 2000) p. 803.
23. *Idem*., in 24th Annual Cocoa Beach Meeting Proceeding, Am. Ceram Soc., Westerville, OH, 2000 (accepted).
24. P. CHRASKA, V. BROZEK, B. J. KOLMAN, J. ILAVSKY, K. NEUFUSS, J. DUBSKY and K. VOLENIK, in "Thermal Spray: Meeting the Challenges of the 21st Century," edited by C. Coddet (ASM International, Materials Park, OH-USA, 1998) p. 1299.
25. J. DUBSKY, B. J. KOLMAN and P. CHRASKA, in "Advances in Thermal Spray Sceince and Technology," edited by C. C. Berndt and S. Sampath (ASM International, Materials Park, OH-USA, 1995) p. 421.
26. L. MUMMERY, "Surface Texture Analysis: The Handbook" (Hommelwerke GmbH, VS-Muhlhausen, West Germany, 1992).
27. J. ILAVSKY, C. C. BERNDT and J. KARTHIKEYAN, *J. Mater. Sci*. **32** (1997) 3925.

Received 10 July 2000
and accepted 27 February 2001